Published in final edited form as:
*Nat Neurosci*. 2008 July ; 11(7): 780–789. doi:10.1038/nn.2146.

# The binding sites for cocaine and dopamine in the dopamine transporter overlap

**Thijs Beuming**[1], **Julie Kniazeff**[2], **Marianne L Bergmann**[2], **Lei Shi**[1,3], **Luis Gracia**[1], **Klaudia Raniszewska**[2], **Amy Hauck Newman**[4], **Jonathan A Javitch**[5], **Harel Weinstein**[1,3], **Ulrik Gether**[2], and **Claus J Loland**[2]

1 *Department of Physiology and Biophysics, Weill Medical College of Cornell University, New York, New York 10021, USA*

2 *Molecular Neuropharmacology Group, Department of Neuroscience and Pharmacology, The Faculty of Health Sciences, The Panum Institute 18.6, University of Copenhagen, Blegdamsvej 3, DK-2200 Copenhagen, Denmark*

3 *Institute for Computational Biomedicine, Weill Medical College of Cornell University, Room E-509, 1300 York Ave., New York, New York 10021, USA*

4 *Medicinal Chemistry Section, Medications Discovery Research Branch, National Institute on Drug Abuse, Intramural Research Program, Department of Health and Human Services, National Institutes of Health, 5500 Nathan Shock Dr., Baltimore, Maryland 21224, USA*

5 *Center for Molecular Recognition and Departments of Psychiatry and Pharmacology, College of Physicians and Surgeons, Columbia University, P&S 11-401, 630 West 168th St., New York, New York 10032, USA*

## Abstract

Cocaine is a widely abused substance with psychostimulant effects that are attributed to inhibition of the dopamine transporter (DAT). We present molecular models for DAT binding of cocaine and cocaine analogs constructed from the high-resolution structure of the bacterial transporter homolog LeuT. Our models suggest that the binding site for cocaine and cocaine analogs is deeply buried between transmembrane segments 1, 3, 6 and 8, and overlaps with the binding sites for the substrates dopamine and amphetamine, as well as for benztropine-like DAT inhibitors. We validated our models by detailed mutagenesis and by trapping the radiolabeled cocaine analog [$^3$H]CFT in the transporter, either by cross-linking engineered cysteines or with an engineered $Zn^{2+}$-binding site that was situated extracellularly to the predicted common binding pocket. Our data demonstrate the molecular basis for the competitive inhibition of dopamine transport by cocaine.

Correspondence should be addressed to U.G. (E-mail: gether@sund.ku.dk).

Note: Supplementary information is available on the Nature Neuroscience website.

**AUTHOR CONTRIBUTIONS**

T.B. designed and performed the computational experiments, analyzed the data and wrote the manuscript draft together with C.J.L. J.K. generated mutants, carried out pharmacological analyses and contributed to the data analysis. M.L.B. and K.R. generated mutants and carried out pharmacological analyses. L.S. contributed to the computational experiments and manuscript refinement. L.G. participated in the design and performance of the computational experiments. A.H.N. contributed with ideas, benztropine analogues and provided expertise in the pharmacology and medicinal chemistry of DAT inhibitors. J.A.J. contributed with ideas and to the design of experiments and writing of the manuscript. H.W. directed the design and performance of the modeling and computational experiments, participated in data analysis and contributed to writing the manuscript. U.G. supervised the project together with C.J.L., designed experiments, analyzed data and wrote the final manuscript. C.J.L. supervised the project together with U.G., designed experiments, generated mutants, performed pharmacological experiments, analyzed data and wrote the manuscript draft together with T.B.

Cocaine is an alkaloid derived from the Peruvian *Erythroxylon coca* plant and has been used as a stimulant for centuries[1]. Today, cocaine is widely abused, especially in the western hemisphere, causing major socioeconomic burdens through increased medical expenses, lost earnings and increased crime[2]. Nonetheless, the molecular mechanisms underlying cocaine's pharmacology and abuse liability are still rather poorly understood.

Earlier correlative studies, as well as studies on genetically modified mice, have suggested that the presynaptic DAT (Fig. 1a) is the primary target for cocaine's action[3–5]. DATmediates reuptake of dopamine from the synaptic cleft and thereby controls the termination of dopaminergic signaling[6–8]. Cocaine is a high-affinity inhibitor of DAT and it is thought that its binding to DAT causes a rapid increase in extracellular dopamine levels that produce the reinforcing effects leading to cocaine abuse[7].

DAT belongs to the neurotransmitter/sodium symporter (NSS, or solute carrier 6) family, together with the closely related transporters for serotonin (SERT) and norepinephrine (NET). NSS proteins couple the transport of $Na^+$ down its concentration gradient with the 'uphill' transport of their respective substrate[7,9–11]. Moreover, several NSS proteins are characterized by co-transport of $Cl^-$ (refs. 7,[9–11]). Recently, the bacterial homolog LeuT, a leucine transporter from *Aquifex aeolicus*, was crystallized and the structure solved at 1.65-Å resolution, providing insight into the tertiary structure of this class of proteins[12]. LeuT has subsequently been crystallized in complex with three different tricyclic antidepressants, clomipramine, imipramine and desimipramine, which target NET and SERT with high affinity and were found to have low affinity for LeuTas well[13,14]. The structures identified an inhibitor-binding site situated in an extracellular vestibule above the substrate-binding site where binding of the inhibitor apparently stabilizes the external gate in a closed conformation, resulting in noncompetitive inhibition of substrate transport[13,14]. The structures raise the question of whether this is a binding mode that can be generalized to the mammalian transporters and to other classes of inhibitors.

Previous mutagenesis studies have attempted to define cocaine-recognition sites in the DAT, resulting in the identification of numerous residues that affect cocaine binding on mutation (for review, see refs. [15,16]). Molecular models of the binding site for cocaine have been proposed on the basis of these data[15,16]; however, in the absence of insight into the accurate tertiary structure of DAT, it has been difficult to differentiate between direct and indirect effects of mutations. Studies using photoreactive cocaine analogs have suggested approximate binding regions in the DAT[17], but without appropriate molecular models it is still difficult to make accurate predictions about the binding site from these data. Thus, the precise nature of the cocaine-binding site and its relationship to the substrate-binding site have remained uncertain.

We present here, on the basis of the LeuT structure and a previously reported sequence alignment[10], molecular models of cocaine and cocaine analog binding to the DAT, in comparison with that of dopamine, amphetamine and DAT inhibitors of the benztropine class. In these models, which were validated by detailed mutagenesis analysis and intramolecular cross-linking strategies, cocaine and its analogs occupy a binding pocket that is deeply buried in the transporter structure, which overlaps with that of dopamine, but is clearly distinct from that observed for antidepressant binding to LeuT.

## RESULTS

### Binding models for dopamine and the cocaine analog CFT

To achieve insight into the molecular basis for the interaction between cocaine and DAT, we developed a molecular model of DAT from the high-resolution structure of the bacterial NSS member LeuT (Protein Data Bank accession code 2A65)[12] and a recently refined alignment

of NSS proteins[10]. The ligand-docking protocol[18] was validated with the successful redocking of leucine into LeuT, which reproduced the crystal structure. Thus, the lowest-energy model identified by the set of criteria established for the docking protocol used throughout had a r.m.s. deviation of ~1 Å relative to the crystal structure. Notably, this low-energy binding mode was populated multiple times during the docking simulation, indicating that the protocol yields converged solutions. Following this same protocol, we determined the binding modes of dopamine and the cocaine analog CFT ((−)-2β-carbomethoxy-3β-(4-fluorophenyl)tropane or WIN 35,428) in the DAT model. CFT has pharmacological properties that are similar to those of cocaine, and was chosen for its high affinity and structural rigidity (Fig. 1b)[19]. The models resulting from the initial docking were refined with molecular dynamics simulations of the complex immersed in an environment that included water and the membrane in explicit atomic details.

The final docking models revealed binding sites for dopamine and CFT in the center of DAT that were composed of residues in transmembrane domains (TMD) 1, 3, 6 and 8. Despite the differences in molecular size and structure between dopamine and CFT, we found that most of the protein side chains that interact with CFT were identical with those in dopamine binding (Fig. 1 and Table 1). A recent modeling study proposed a similar binding mode for dopamine[20]. The protonated amine of dopamine formed a salt-bridge with the Asp79 side chain (Fig. 1c). Our models also predicted a polar interaction between the amine of CFT and Asp79 (Fig. 1d). The aromatic ring of dopamine and the tropane ring of CFT interacted with hydrophobic and aliphatic residues in TMD 1 (Phe76), 3 (Val152) and 6 (Phe320 [omitted for clarity], Phe326, Val328) (Fig. 1c,d). Dopamine further engaged in hydrogen bonds with exposed backbone carbonyls of the unwound regions of TMDs 1 and 6 (Fig. 1c and Table 1) and the *N*-methyl substituent of CFT was inserted in between TMDs 1 and 6, where it interacted with Phe76 and with the backbone of TMD 6 (Fig. 1d and Table 1). The para-hydroxyl group of the catechol ring in dopamine interacted the with backbone atoms of Ser149 and Val152, whereas the meta-hydroxyl group interacted with Ser422, Ala423 and G425. In the case of CFT, these residues interacted with the halogenated phenyl ring (Fig. 1c,d and Table 1).

Important differences also became apparent in the binding sites of the two ligands. One marked difference involved the network of interactions surrounding Tyr156 in TMD 3. Notably, this residue is 100% conserved in all NSS transporters[10], and, in LeuT, the hydroxyl group of the tyrosine binds the carboxylate group of leucine[12]. In the dopamine-binding model, the network of interactions involving Tyr156 included an aromatic-aromatic stacking interaction with the catechol ring of dopamine, a hydrogen bond between the hydroxyl group and Asp79 in TMD 1 and a hydrophobic-aromatic interaction with the side chain of Leu80 on the extracellular side (Fig. 1c). CFTalso interacted with Tyr156 through the 2β-methylester substituent (Fig. 1d) in the CFT-binding model, but stabilized a different conformation of the side chain. This reorientation disrupted the hydrogen bond between Tyr156 and the key Asp79 residue (Fig. 1c,d). Another key difference between CFT and dopamine binding involved a unique interaction between the nitrogen of Asn157 and the fluoride atom of CFT (Fig. 1d and Table 1).

## Experimental validation of binding models

We sought to experimentally validate the binding models of CFT and dopamine by verifying commonalities and differences between their binding modes. Previous reports have suggested a role for Asp79 in binding both CFT and dopamine[21,22], which is consistent with the interactions that we observed between the protonated amines of the ligands and this residue (Fig. 1c,d). Further supporting our model, earlier studies of DAT have indicated that Phe76, Phe320 and Phe326 (ref. 23) are involved in the binding. Val152, Tyr156, Val328 and Ser422

(Table 1) were also predicted to be involved in binding both CFT and dopamine, and we decided to analyze them in further detail.

In TMD 3, Val152 is predicted to form hydrophobic interactions with dopamine and CFT (Fig. 1c,d). It has been suggested previously that this residue is involved in cocaine binding from analysis of bovine and human DAT chimeras[24] and by analysis of the corresponding residue in SERT (Ile172)[25]. To further assess the role of this position in DAT, we mutated the residue to alanine (V152A), isoleucine (V152I) and methionine (V152M). Consistent with our predictions, the $K_M$ value for [$^3$H]dopamine uptake increased 5–18-fold in these mutants (Fig. 2a and Supplementary Table 1 online). Moreover, consistent with a role of this residue in binding both dopamine and CFT, the $K_D$ value for [$^3$H]CFT binding increased 2–4-fold in V152A and V152I, and we were unable to measure binding in V152M, suggesting a larger loss of binding affinity (Supplementary Table 1). The [$^3$H]dopamine uptake–inhibition assay confirmed that there was a more pronounced effect on CFT binding of the methionine substitution as compared with V152A and V152I (Fig. 2b and Supplementary Table 1). For Tyr156, which is situated one α-helical turn above Val152 in TMD 3, our models predicted an essential role for the aromatic ring in binding both dopamine and CFT (Fig. 1c,d). Correspondingly, mutation of Tyr156 to Ala (Y156A) and Cys (Y156C) resulted in inactive transporters with neither measurable [$^3$H]dopamine uptake nor [$^3$H]CFT binding (data not shown). Surface biotinylation and immunofluorescence experiments showed similar plasma membrane expression of Y156C compared to controls (Supplementary Fig. 1 online). Thus, the lack of measurable binding and uptake was probably the result of disruption of critical interactions with the ligands and not of impaired folding and retention in the endoplasmic reticulum. Note that previous studies in SERT and in the GABA transporter-1 (GAT-1) have suggested that this highly conserved tyrosine is involved in substrate binding in these transporters as well[26,27].

According to our model, Val328 in TMD 6 is another important residue in the hydrophobic pocket that surrounds the ligands, and thus its mutation would be predicted to affect both recognition of CFT and dopamine (Fig. 1c,d). Consistent with this prediction, we could not measure [$^3$H]CFT binding on mutation of Val328 to isoleucine (V328I; data not shown). This was supported by [$^3$H]dopamine uptake–inhibition assays showing more than tenfold loss in CFT potency (Fig. 2b and Supplementary Table 1). In contrast, we did not observe an effect on the $K_M$ value for [$^3$H]dopamine uptake in the V328I construct, but the $V_{MAX}$ value was substantially decreased (Fig. 2a and Supplementary Table 1), whereas a less conservative substitution (V328F) made [$^3$H]dopamine uptake and [$^3$H]CFT binding unmeasurable (data not shown). The differences in effects of V328I on dopamine and CFT recognition were analyzed in the structural context with molecular dynamics simulations of the V328I mutant. We found that dopamine could accommodate the added bulk in V328I through a small shift in the position of the ligand that was made possible by its relatively small size; in contrast, CFT occupied a larger portion of the binding-site volume, and its interactions did not permit such a shift to avoid the steric clash (data not shown).

Finally, we analyzed Ser422 (situated in TMD 8), which, according to our model, interacts with the hydroxyls of the catechol ring in dopamine and the aromatic ring in CFT (Fig. 1c,d and Table 1). Substitution with alanine (S422A) increased the $K_M$ value for [$^3$H]dopamine uptake ~fivefold and decreased CFT inhibition potency by 30-fold (Fig. 2a,b and Supplementary Table 1). Consistent with the model, we did not detect [$^3$H]CFT binding in S422A (data not shown). In summary, by showing effects on both dopamine and CFT recognition, the mutational analysis of Val152, Tyr156, Val328 and Ser422 supports our binding models and, thus, an overlapping binding site for these compounds in DAT.

To investigate the predicted differences between the binding modes of dopamine and CFT, we also mutated Tyr156 to phenylalanine (Y156F). The removal of this hydroxyl group would be predicted to destabilize the dopamine-binding pocket by disrupting the hydrogen bond between Tyr156 and Asp79, while preserving the CFT binding scheme in which this hydrogen bond is already missing (Fig. 1c,d). Consistent with this, the $K_M$ value for [3H]dopamine uptake was markedly increased in Y156F and the $V_{MAX}$ for [3H]dopamine uptake was markedly decreased (Fig. 2c–f and Supplementary Table 2 online). We also observed a decrease in estimated dopamine affinity (~13-fold) in [$^3$H]CFT competition binding experiments (Supplementary Table 3 online). In contrast, we observed no measurable change in CFT affinity as determined by direct [$^3$H]CFT binding and by measuring inhibition of [$^3$H]dopamine uptake (Fig. 2c–f and Supplementary Tables 2 and 3).

In the dopamine-binding model, Tyr156 not only formed a hydrogen bond with Asp79, but also made a hydrophobic-aromatic interaction with Leu80 in TMD 1 (Fig. 1c). Accordingly, we predicted that mutation of Leu80 would destabilize Tyr156, and thereby selectively impair the interaction of DAT with dopamine, as in Y156F. Indeed, mutation of Leu80 to Cys (L80C) decreased the potency of dopamine, whereas [$^3$H]CFT binding was unaffected (Supplementary Fig. 2 and Supplementary Table 4 online). [$^3$H]dopamine uptake was not measurable in L80C (data not shown), which is consistent with the decreased potency of dopamine to inhibit [$^3$H]CFT binding, but which also suggests an additional effect on uptake efficacy as compared with Y156F. Note that mutation in SERT and GAT-1 of the residues corresponding to Leu80 also resulted in marked impairment of substrate transport, supporting a possible general role of this position in NSS proteins[28,29].

As a final test to validate the differences between the dopamine- and CFT-binding modes, we mutated Asn157 in TMD 3, which forms a polar interaction with the fluorine substituent of CFT and therefore has the only predicted unique side chain interaction with this compound compared with the dopamine-binding mode (Fig. 1d and Table 1). Indeed, the mutation (N157C) did not affect the $K_M$ value for [$^3$H]dopamine uptake, but the $K_D$ for [$^3$H]CFT binding was increased by ~15-fold, supporting the specific interaction in the model (Fig. 2c–f and Supplementary Table 1).

## A buried CFT-binding pocket is supported by cross-linking

To exclude indirect effects from the inferences suggested by the mutagenesis and to further validate the buried position of the CFT binding site, we attempted to trap radiolabeled CFT in its binding pocket by introducing structural constraints at positions predicted to lie extracellular to the bound ligand. First, we undertook to engineer a $Zn^{2+}$-binding site, as such constructs have been used previously to impose intramolecular structural constraints in membrane proteins, including this transporter class[30–32]. Our model predicted that a bidentate (two coordinating residues) $Zn^{2+}$-binding site might be formed above the CFT binding pocket between position 80 (Leu80) and 159 (Ile159) if these positions were substituted with a histidine and a cysteine, respectively (Fig. 3a). According to the model, $Zn^{2+}$ would coordinate His80 and Cys159 in a tetrahedral conformation with Cys-S–to-$Zn^{2+}$ distances of 2.6 Å, and His-N–to-$Zn^{2+}$ distances of 2.2 Å. Binding of $Zn^{2+}$ to this site should constrain the His80 side chain and place the imidazole ring immediately above the CFT-binding pocket, thereby potentially restricting release of bound CFT (Fig. 3a). It is interesting to note that the $Zn^{2+}$-binding site position corresponded to an extracellular vestibule that was recently shown to represent a noncompetitive binding site for antidepressants in LeuT[13,14] (illustrated by a spherical model of clomipramine bound to LeuT; Fig. 3a). Thus, the two residues in LeuT corresponding to Leu80 and Ile159 (Leu25 and Ile111) both line this allosteric site[13,14], making the binding of $Zn^{2+}$ and of the antidepressant mutually exclusive (Fig. 3a).

To validate the model experimentally, we generated the $Zn^{2+}$-binding double mutant L80H-I159C in a DAT background (E2C H193K) in which endogenous $Zn^{2+}$ sensitivity was eliminated by mutation of His193 to lysine[30,33]. Two extracellular cysteines (Cys90 and Cys306) were also mutated in this construct, thereby rendering the transporter insensitive to modification with extracellularly applied sulfhydryl-reactive reagents[33]. This background was chosen to allow direct comparison with the cysteine cross-linking experiments described below (see Supplementary Note online). Consistent with the model, application of 100 μM $Zn^{2+}$ to cells expressing the resulting construct E2C H193K–L80H-I159C caused a decrease in the off rate of prebound [$^3$H]CFT by ~fourfold (Fig. 3a). In contrast, $Zn^{2+}$ had no effect on [$^3$H]CFT dissociation in the background construct (E2C H193K) or in the following control mutants L80H, I159C, L80H-I159A and L80K-I159C (all made in E2C H193K) (Fig. 3a). Unfortunately, we were unable to perform uptake experiments in E2C H193K–L80H-I159C because of the importance of Leu80 for dopamine binding (Supplementary Table 4). Note, however, that $Zn^{2+}$ did not affect [$^3$H]CFT binding affinity *per se* ($K_D$ = 3.1 [2.4, 4.1] nM with $Zn^{2+}$ versus 3.4 [2.7, 4.2] nM without $Zn^{2+}$, means with calculated s.e.m. interval in square brackets, $n$ = 3 and 8, respectively). Thus, the decreased off rate cannot be the result of stabilizing the transporter in a high-affinity [$^3$H]CFT conformation, but rather is the result of steric occlusion of a buried binding site with the $Zn^{2+}$ ion affecting both the on and off rates. This was confirmed in on-rate experiments showing that the rate of [$^3$H]CFT binding to E2C L80H-I159C-H193K was decreased ~threefold in the presence of $Zn^{2+}$ ($k_{0.5}$ = 15.4 [13.6, 17.9] min with 100 μM $Zn^{2+}$ versus 5.8 [5.3, 6.4] without $Zn^{2+}$ (95% confidence interval, $n$ = 2)).

In a second strategy we used the bifunctional sulfhydryl-reactive cross-linking reagent 1,3-propanediyl bismethane-thiosulfonate (MTS-3-MTS) to crosslink cysteine residues with Cβ atoms separated by <10 Å. We introduced cysteines in the background construct E2C (see Supplementary Note) at positions 84 (Trp84) and 159 (Ile159), which would be just above the CFT binding site with a predicted distance of 8.5 Å between the Cβ atoms of Cys84 and Cys159 (Fig. 3b). In addition, these positions have been cross-linked in the related GAT-1 (ref. 34). We observed a >threefold decrease in [$^3$H]CFT off-rate on treatment of the resulting double mutant E2C W84C-I159C with 0.5 mM MTS-3-MTS after prebinding of [$^3$H]CFT (Fig. 3b), consistent with cross-linking of the two engineered cysteines and subsequent partial trapping of [$^3$H]CFT in its binding site. There was no effect of MTS-3-MTS on [$^3$H]CFT dissociation in the background construct E2C or in the control mutants W84C, I159C, W84C-I159A or W84A-I159C (all made in E2C; Fig. 3b). We also attempted cross-linking in E2C W84C-I159C mutants with copper phenanthroline and cadmium; however, we did not observe an effect of these, suggesting that the two cysteines did not come sufficiently close to form a disulfide bridge or to be cross-linked by cadmium. Finally, we used the bulky MTS reagent benzocaine-methanethiosulfonate (BZ-MTS) to test whether imposing a simple steric hindrance above the binding pocket was sufficient to slow [$^3$H]CFT dissociation (Fig. 3c). Consistent with this notion, BZ-MTS (0.5 mM) markedly decreased the off-rate of prebound [$^3$H]CFT in both E2C I159C and in E2C W84C (Fig. 3c), whereas no effect on [$^3$H]CFT dissociation was observed in the background construct E2C or in the control mutants I159A or W84A (both made in E2C; Fig. 3c). Although the effect of the reagents on CFT dissociation was similar to that of $Zn^{2+}$, we were unable to reliably assess the effect of MTS-3-MTS and BZ-MTS pretreatment on [$^3$H]CFT association because of interference from cysteines still present in the E2C background (Supplementary Note).

## Binding modes for cocaine, amphetamine and benztropines

The binding models of CFT and dopamine were first compared with that of cocaine, which was predicted to bind similarly to CFT (Fig. 4). Consistent with this, we observed no changes in affinity for cocaine in Y156F as determined in [$^3$H]CFT competition binding experiments and [$^3$H]dopamine uptake–inhibition experiments, as predicted by the disruption of the Tyr156-

Asp79 hydrogen bond by cocaine binding (Fig. 4a and Supplementary Tables 2 and 3). This similarity in binding modes was further supported measurements of the ability of cocaine to inhibit [$^3$H]dopamine uptake in V152M, V328I and S422A mutants (Supplementary Table 1). Mutation of Asn157 (N157C) also affected cocaine binding (fivefold decrease in potency; Supplementary Table 1); however, the interaction of CFT was through the fluorine substituent (Fig. 1d), whereas the interaction of cocaine was through the aromatic ring (Fig. 4a). Calculation of the nonbonded interaction energy between the side chain of Asn157 and the ligands agreed with these data, with CFT showing a favorable interaction energy of ~1.9 kcal mol$^{-1}$, cocaine showing 0.8 kcal mol$^{-1}$ and dopamine having virtually no interaction (~0.1 kcal mol$^{-1}$).

We also compared the binding models of dopamine, CFT and cocaine with those of a series of structurally diverse DAT ligands (Fig. 5a). We found it interesting that the Tyr156-Asp79 hydrogen bond that we observed in dopamine binding was preserved in all modeled complexes except those of cocaine and CFT (Fig. 4 and Supplementary Fig. 3 online). Accordingly, it would be expected that the removal of the hydrogen bond by mutation of Tyr156 to phenylalanine would affect binding for all these ligands, as we observed for dopamine. Consistent with this, we observed, on the basis of [$^3$H]CFT competition binding experiments, 19- and 6-fold decreases in affinity for the substrates amphetamine and 3,4-methylenedioxy-*N*-methylamphetamine (‘ecstasy’), respectively (Fig. 4d, Supplementary Fig. 3 and Supplementary Table 4). For three different benztropines, including benztropine itself, JHW007 and MFZ 2-71 (refs. 35,[36]), the experimental observations were also consistent with the models; hence, the binding affinities assessed in [$^3$H]CFT competition assays decreased between 7- and 35-fold for the three compounds on mutation of Tyr156 to phenylalanine, supporting the idea that the Asp79-Tyr156 hydrogen bond is important for interaction (Fig. 4f, Supplementary Fig. 3 and Supplementary Table 3). The analog JHW007 was of particular interest to us, as it has been shown to fully antagonize the response to cocaine in behavioral models[36]. Note that we observed mainly similar effects when assessing [$^3$H]dopamine uptake–inhibition potency in Y156F as compared with calculating affinity from [$^3$H]CFT competition binding, although the effects appeared to be more modest for MFZ 2-71 and methylenedioxy-*N*-methylamphetamine (Supplementary Tables 2 and 3).

The stability and time-dependent behavior of the discriminant Tyr156-Asp79 hydrogen bond was explored with molecular dynamics simulations. All of the modeled complexes were simulated for 1 ns at 310 K, and the average distance between the oxygen atoms of Tyr156 and Asp79 was monitored in the second (500 ps) half of the trajectory. As illustrated by plotting the observed affinity ratios ($K_I$ of Y156F:$K_I$ of wild type) against the donor-acceptor distance of the hydrogen-bond (Fig. 5b), the hydrogen bond was continuously present (distance <3.5 Å) in all trajectories, except for those of CFT and cocaine, in agreement with the inference from experimental data. Finally, the CFT and dopamine models were simulated in a realistic solvated membrane environment, showing that disruption of the Tyr156-Asp79 hydrogen bond was associated with water permeating deep into the CFT-binding site (Fig. 5c). In the dopamine-bound state, however, the Tyr156-Asp79 hydrogen bond effectively closed the binding site from the extracellular side and prevented water from entering (Fig. 5c). Notably, the increased hydration stabilized the CFT-binding site and thereby compensated for the loss of intramolecular interactions. This explains mechanistically the unaltered affinity of CFT seen on removal of the Tyr156-Asp79 hydrogen bond in Y156F, and also suggests how the recently shown ability of cocaine and CFT, but not dopamine, to stabilize an open, outward-facing conformation of the transporter can be achieved[37].

## DISCUSSION

The molecular mode of interaction of cocaine with DAT has long been the subject of speculation[7,15,16]. In particular, it has been debated whether or not the cocaine-binding site in DAT overlaps with that of dopamine. If inhibition of dopamine uptake by cocaine is the result of an allosteric mechanism, it would be possible, at least in theory, to generate a cocaine antagonist for treatment of cocaine addiction that might block cocaine binding without affecting dopamine transport[38]. However, if the binding sites for the two compounds are overlapping, then the challenge would be greater, and of a different nature. In support of an allosteric mechanism, previous studies have identified several residues, which, on mutation, generate differentiated effects on cocaine and dopamine binding[5,15,16,33,38]. One study supporting an allosteric mechanism showed that mutation of three residues in the external part of TMD 2 results in a cocaine-insensitive DAT that is still capable of transporting dopamine[39]. However, an analysis of the LeuT structure suggested that the cocaine antagonizing effects of these mutations were probably the result of conformational changes in TMD 2, which indirectly might affect its binding to another site, such as the canonical substrate-binding site[40]. Of further interest, we previously identified a mutation (Y335A) in DAT that leads to a >100-fold decrease in cocaine affinity, while causing an increase in dopamine affinity[41]. Nonetheless, experimental data, as well as the fact that the residue is located in an intracellular loop, strongly suggest that the marked decrease in affinity for cocaine and analogs is the result of an altered conformational equilibrium of DAT toward an inward facing conformation, rather than because of disruption of a direct interaction between the mutated residue and the ligand[33].

The bacterial NSS member LeuTwas recently crystallized in complex with three different antidepressants, clomipramine, imipramine and desipramine[13,14]. These compounds show low affinity for the LeuT, in addition to being potent inhibitors of SERT and/or NET, which are closely related to DAT[8]. The new LeuT structures identified a non-competitive binding site for the antidepressants in an extracellular-facing vestibule situated above the occluded substrate-binding site, where the compounds are thought to stabilize the external gate in a closed conformation, and thereby noncompetitively inhibit substrate transport[13,14]. The new structures raised the question of whether they describe a binding mode for inhibitors that can be generalized to mammalian NSS proteins, as well as to other classes of NSS inhibitors such as cocaine. Hence, the allosteric nature of anti-depressant binding to LeuTrenewed interest in an allosteric mechanism for cocaine in DAT.

Our current findings strongly argue against this possibility by showing clear evidence that cocaine and related inhibitors do not bind in the vestibule occupied by antidepressants in LeuT. Instead, our data suggest a binding site for cocaine and its analogs that is buried deep in between TMDs 1, 3, 6 and 8, and that overlaps extensively with that of dopamine (Fig. 1 and Table 1). Our ligand-binding models were substantiated by mutation of residues predicted to interact with both ligands, as well as of residues predicted to selectively interact with either dopamine or cocaine/CFT. The buried nature of the cocaine/CFT-binding site was further confirmed by the effects of chemical cross-links or of steric block at engineered positions aligned with those that form the noncompetitive binding site for antidepressants in LeuT (Fig. 3). It is noteworthy that not all mutations in the transmembrane core affected dopamine and/or cocaine/CFT binding. For example, mutation of Ile159 right above the binding site did not affect the $K_M$ value for [$^3$H]dopamine uptake or the $K_D$ value for [$^3$H]CFT binding (Supplementary Table 4), lending additional support to the specificity of our observations. In addition, we mutated Leu147 (L147C), positioned in TMD 3, right below the binding site, without observing any change in either dopamine or CFT affinity (data not shown). Previous studies using photoreactive cocaine analogs are consistent with our data. Recently, it was shown that the photoreactive cocaine analog [$^{125}$I]RTI 82 incorporated into TMD 6 (ref. 17), which is an

important part of the cocaine-binding site in the models presented here. Together with these previous findings, our results provide strong evidence that cocaine and its analogs are true competitive inhibitors. It is interesting to note that the binding site in SERT for cocaine is probably similar to that seen in DAT. Mutation of Asp98 in SERT to glutamate (corresponding to Asp79 in TMD 1 of DAT), for example, markedly impairs cocaine binding[42]. Similarly, it has been shown that mutation of Ile172 in SERT (Leu152 in DAT) markedly decreases cocaine affinity[25,26], paralleling our observations in the corresponding DAT mutation (Fig. 2a,b).

Molecular models of DAT with dopamine or cocaine bound have been generated before the LeuT structure became available. These models were constructed either by positioning the twelve predicted helices relative to one another on the basis of information from existing mutagenesis data or by using available projection structures of other transport proteins, such as the *E. Coli* $Na^+/H^+$ exchanger NhaA[43,44]. Consistent with the present findings, these models predicted the existence of a central hydrophobic cavity harboring the cocaine- and dopamine-binding sites. Some residues that were shown in this study to interact with the ligands were also suggested to interact in these earlier models. Specifically, Asp79 in TMD 1 was predicted to form an ionic interaction with the protonated amine of dopamine, as well as with the amine of CFT/cocaine[43]. Moreover, Phe76 was predicted to line the hydrophobic binding cavity[23,43]. Nonetheless, there are also substantial differences, with several interactions diverging between the earlier models and our present LeuT-based models. These differences are not surprising given the major differences between the structural organization of LeuT and, for example, NhaA; hence, although this protein is also a 12-transmembrane segment ion-coupled transport protein, it is not as valid a template for modeling of DAT or other mammalian NSS proteins as LeuT. In conclusion, accurate mapping of the cocaine- and dopamine-binding sites in DAT has not been feasible before the LeuT structure became available as a modeling template.

We modeled and analyzed inhibitors of the benztropine class. These inhibitors were also suggested to bind in the central cavity, and thus to a binding site overlapping with that of dopamine. In contrast to cocaine/CFT, however, they bound in a way that preserved the Asp79-Tyr156 hydrogen bond, and thereby formed a closed binding pocket. Notably, we have recently assessed conformational changes in DAT promoted by different benztropine and cocaine analogs by determining reactivity of a cysteine inserted in position 159, which is believed to be accessible in the outward facing conformation when the extracellular gate is open and inaccessible when the gate is closed[37]. These data showed that, although cocaine and its analogs probably stabilize the open outward-facing conformation, benztropines probably stabilize the closed conformation. This is consistent with the present binding models and is supported by simulations of the CFT binding model in a realistic membrane environment showing water permeating deep into the CFT-binding site (Fig. 5). Of note, several benztropine analogs are less effective than cocaine as behavioral stimulants, despite having similar or higher affinity and selectivity for the DAT than cocaine[36,45]. Furthermore, one of the benztropines, JHW 007, was found to potently antagonize the behavioral effects of cocaine[36]. It is tempting, therefore, to speculate that the different binding configurations between cocaine and benztropines could contribute to their different pharmacological profiles, and therefore offer structure-informed hypotheses for molecular mechanisms underlying psychostimulant action.

In summary, we present here, to the best of our knowledge, the first comprehensive and experimentally validated model of substrate and inhibitor binding to the DAT, in the context of the high-resolution structure of the bacterial transporter homolog LeuT. Our data provide strong evidence that substrates and inhibitors, including widely abused psychostimulants such as cocaine and amphetamine, occupy an essentially similar binding pocket that is buried deep in the DAT molecule and corresponds to the substrate-binding site in the LeuT structure. These

data therefore finally close the door to the possibility of generating a competitive inhibitor of cocaine binding that treats cocaine addiction without itself inhibiting dopamine uptake.

## METHODS

### Modeling of DAT and ligand complexes

Our modeling protocol is described in detail in the Supplementary Methods online. Briefly, ligands were docked to the LeuT-based model using a simulated annealing–based protocol[18], implemented in CHARMM[46]. Initial positions were generated with a Monte Carlo algorithm. Parameters for the ligands were generated with structures from the Cambridge Structure Database and *ab initio* calculations at the HF/6-31G* level. The restrained electrostatic potential–fit method[47] was used to derive the atomic charges. Ligand-transporter interactions were assessed by simulating the complexes in a realistic membrane environment model for ~50 ns (Supplementary Methods).

### Modeling of chemical cross-links

The $Zn^{2+}$-binding site was modeled in I159C-L80H and the side chains were optimized using the rotamer-optimization module of InsightII (Accelrys). $Zn^{2+}$ was initially placed in between the Cys-S and His-N atoms and the complex was minimized for 1,000 steps, without any restraints on $Zn^{2+}$. The ε-rotameric state of His80 produced the most stable complex. For the BZ-MTS and MTS-3-MTS models, mutants I159C and W84C-I159C were generated in the DAT model, respectively. The structure of BZ-MTS was built in an extended fashion and covalently linked to I159C. Torsional angles of the I159C/BZ-MTS unit were modified to minimize steric overlap with other residues. The MTS-3-MTS molecule was placed in between the rotamer-optimized Cys84 and Cys159 by minimizing the distance between the sulfur atoms of extended MTS-3-MTS and Cys84/Cys159. The BZ-MTS and MTS-3-MTS complexes were minimized to generate the final models.

### Molecular biology

Synthetic cDNAs encoding the human DAT (synDAT) and E2C were subcloned into pcDNA3 (Invitrogen)[33]. All mutations were generated by the QuickChange method (Stratagene) and confirmed by DNA sequencing.

### Cell culture and transfection

COS7 cells were grown as described previously and transiently transfected with wild-type and mutant constructs using the calcium phosphate–precipitation method[33].

### [$^3$H]Dopamine-uptake experiments

Uptake assays were carried out as described previously[33] using 2,5,6-[$^3$H]dopamine (9–13 Ci $mmol^{-1}$, Amersham Pharmacia Biotech), and transfected COS7 cells were plated in either 24-well ($10^5$ cells per well) or 12-well dishes ($3 \times 10^5$ cells per well). The uptake assays were carried out 2 d after transfection for 5 min at room temperature (20–22 °C) in uptake buffer (25 mM HEPES, 130 mM NaCl, 5.4 mM KCl, 1.2 mM $CaCl_2$, 1.2 mM $MgSO_4$, 1 mM L-ascorbic acid, 5 mM D-glucose and 1 μM of the catechol-*O*-methyltransferase inhibitor Ro 41-0960 (Sigma), pH 7.4).

### [$^3$H]CFT-binding experiments

Binding assays were carried out on intact COS7 cells as described previously[30] using 2–4 nM [$^3$H]CFT (WIN 35,428 from PerkinElmer, 87 Ci $mmol^{-1}$) as a radioligand. The assay was performed 2 d after transfection in uptake buffer on cells in either 24-well ($10^5$ cells per well) or 12-well ($3 \times 10^5$ cells per well).

### [$^3$H]CFT off-rate experiments

Binding of [$^3$H]CFT to transfected COS7 cells was initiated by the addition of 4 nM [$^3$H]CFT in 450 μl of uptake buffer, and the cells were kept at 4 °C. After 1 h, either $Zn^{2+}$ (100 μM), MTS-3-MTS (0.5 mM) or BZ-MTS (0.5 mM) were added and the plates were incubated for 10 min at 21 °C before washing twice in uptake buffer (21 °C). At $t$ = 0, 0.5 ml of uptake buffer (21 °C) with 100 μM CFT (for the $Zn^{2+}$ experiments, the uptake buffer also contained 100 μM $Zn^{2+}$) were added and the reaction was stopped by aspiration of uptake buffer at the indicated time points. Cells were lysed and counted as described previously[30].

### [$^3$H]CFT on-rate experiments

Transfected cells were washed and preincubated with buffer or $Zn^{2+}$ (100 μM) before the addition of [$^3$H]CFT. The [$^3$H]CFT incubations were stopped at the indicated time points, washed twice in ice cold uptake buffer, transferred and counted as described previously[30].

### Data calculations

Data from uptake and binding experiments were analyzed by nonlinear regression analysis using Prism 5.0 (GraphPad Software). The $IC_{50}$ values used in the estimation of $K_M$ values for [$^3$H]dopamine uptake and $K_D$ values for [$^3$H]CFT binding were calculated from means of the obtained $pIC_{50}$ values and the s.e. interval from the $pIC_{50}$ ± s.e.m. values. The $K_I$ values were calculated from the $IC_{50}$ values using the equation $K_I = IC_{50}/(1+(L/K_M))$ for [$^3$H]dopamine uptake and $K_I = IC_{50}/(1+(L/K_D))$ for [$^3$H]CFT binding ($L$ = concentration of [$^3$H]dopamine or [$^3$H]CFT).

## Supplementary Material

Refer to Web version on PubMed Central for supplementary material.

## Acknowledgments

We thank P. Elsman and D. Vang Larsen for excellent technical assistance. The work was supported in part by US National Institute of Health Grants P01 DA 12408 (U.G., H.W. and J.A.J.) and DA 22413 (J.A.J.), the Danish Medical Research Council (C.J.L., J.K. and U.G.), the Lundbeck Foundation (C.J.L. and U.G.), the Novo Nordisk Foundation (M.L.B., C.J.L., J.K. and U.G.), the Maersk Foundation (C.J.L.) and the US National Institute on Drug Abuse Intramural Research Program (A.H.N.). J.K. was a recipient of a European Molecular Biology Organization long-term fellowship.

## References

1. Aguayo LG, et al. Historical and current perspectives of neuroactive compounds derived from Latin America. Mini Rev Med Chem 2006;6:997–1008. [PubMed: 17017999]
2. Nnadi CU, Mimiko OA, McCurtis HL, Cadet JL. Neuropsychiatric effects of cocaine use disorders. J Natl Med Assoc 2005;97:1504–1515. [PubMed: 16334497]
3. Ritz MC, Lamb RJ, Goldberg SR, Kuhar MJ. Cocaine receptors on dopamine transporters are related to self-administration of cocaine. Science 1987;237:1219–1223. [PubMed: 2820058]
4. Giros B, Jaber M, Jones SR, Wightman RM, Caron MG. Hyperlocomotion and indifference to cocaine and amphetamine in mice lacking the dopamine transporter. Nature 1996;379:606–612. [PubMed: 8628395]
5. Chen R, et al. Abolished cocaine reward in mice with a cocaine-insensitive dopamine transporter. Proc Natl Acad Sci USA 2006;103:9333–9338. [PubMed: 16754872]
6. Torres GE, Amara SG. Glutamate and monoamine transporters: new visions of form and function. Curr Opin Neurobiol 2007;17:304–312. [PubMed: 17509873]
7. Gether U, Andersen PH, Larsson OM, Schousboe A. Neurotransmitter transporters: molecular function of important drug targets. Trends Pharmacol Sci 2006;27:375–383. [PubMed: 16762425]

8. Iversen L. Neurotransmitter transporters and their impact on the development of psychopharmacology. Br J Pharmacol 2006;147(Suppl 1):S82–S88. [PubMed: 16402124]
9. Chen NH, Reith ME, Quick MW. Synaptic uptake and beyond: the sodium- and chloride-dependent neurotransmitter transporter family SLC6. Pflugers Arch 2004;447:519–531. [PubMed: 12719981]
10. Beuming T, Shi L, Javitch JA, Weinstein H. A comprehensive structure-based alignment of prokaryotic and eukaryotic neurotransmitter/$Na^+$ symporters (NSS) aids in the use of the LeuT structure to probe NSS structure and function. Mol Pharmacol 2006;70:1630–1642. [PubMed: 16880288]
11. Zomot E, et al. Mechanism of chloride interaction with neurotransmitter:sodium symporters. Nature 2007;449:726–730. [PubMed: 17704762]
12. Yamashita A, Singh SK, Kawate T, Jin Y, Gouaux E. Crystal structure of a bacterial homologue of $Na^+/Cl^-$-dependent neurotransmitter transporters. Nature 2005;437:215–223. [PubMed: 16041361]
13. Zhou Z, et al. LeuT-desipramine structure reveals how antidepressants block neurotransmitter reuptake. Science 2007;317:1390–1393. [PubMed: 17690258]
14. Singh SK, Yamashita A, Gouaux E. Antidepressant binding site in a bacterial homologue of neurotransmitter transporters. Nature 2007;448:952–956. [PubMed: 17687333]
15. Uhl GR, Lin Z. The top 20 dopamine transporter mutants: structure-function relationships and cocaine actions. Eur J Pharmacol 2003;479:71–82. [PubMed: 14612139]
16. Volz TJ, Schenk JO. A comprehensive atlas of the topography of functional groups of the dopamine transporter. Synapse 2005;58:72–94. [PubMed: 16088952]
17. Vaughan RA, et al. Localization of cocaine analog [125I]RTI 82 irreversible binding to transmembrane domain 6 of the dopamine transporter. J Biol Chem 2007;282:8915–8925. [PubMed: 17255098]
18. Niv MY, Weinstein H. A flexible docking procedure for the exploration of peptide binding selectivity to known structures and homology models of PDZ domains. J Am Chem Soc 2005;127:14072–14079. [PubMed: 16201829]
19. Carroll FI, Lewin AH, Boja JW, Kuhar MJ. Cocaine receptor: biochemical characterization and structure-activity relationships of cocaine analogues at the dopamine transporter. J Med Chem 1992;35:969–981. [PubMed: 1552510]
20. Huang X, Zhan CG. How dopamine transporter interacts with dopamine: insights from molecular modeling and simulation. Biophys J 2007;93:3627–3639. [PubMed: 17704152]
21. Kitayama S, et al. Dopamine transporter site-directed mutations differentially alter substrate transport and cocaine binding. Proc Natl Acad Sci USA 1992;89:7782–7785. [PubMed: 1502198]
22. Ukairo OT, et al. Recognition of benztropine by the dopamine transporter (DAT) differs from that of the classical dopamine uptake inhibitors cocaine, methylphenidate, and mazindol as a function of a DAT transmembrane 1 aspartic acid residue. J Pharmacol Exp Ther 2005;314:575–583. [PubMed: 15879005]
23. Lin Z, Wang W, Kopajtic T, Revay RS, Uhl GR. Dopamine transporter: transmembrane phenylalanine mutations can selectively influence dopamine uptake and cocaine analog recognition. Mol Pharmacol 1999;56:434–447. [PubMed: 10419565]
24. Lee SH, et al. Importance of valine at position 152 for the substrate transport and 2β-carbomethoxy-3β-(4-fluorophenyl)tropane binding of dopamine transporter. Mol Pharmacol 2000;57:883–889. [PubMed: 10779370]
25. Henry LK, et al. Tyr-95 and Ile-172 in transmembrane segments 1 and 3 of human serotonin transporters interact to establish high-affinity recognition of antidepressants. J Biol Chem 2006;281:2012–2023. [PubMed: 16272152]
26. Chen JG, Sachpatzidis A, Rudnick G. The third transmembrane domain of the serotonin transporter contains residues associated with substrate and cocaine binding. J Biol Chem 1997;272:28321–28327. [PubMed: 9353288]
27. Bismuth Y, Kavanaugh MP, Kanner BI. Tyrosine 140 of the gamma-aminobutyric acid transporter GAT-1 plays a critical role in neurotransmitter recognition. J Biol Chem 1997;272:16096–16102. [PubMed: 9195904]

28. Henry LK, Adkins EM, Han Q, Blakely RD. Serotonin and cocaine-sensitive inactivation of human serotonin transporters by methanethiosulfonates targeted to transmembrane Domain I. J Biol Chem 2003;278:37052–37063. [PubMed: 12869570]
29. Zhou Y, Bennett ER, Kanner BI. The aqueous accessibility in the external half of transmembrane domain I of the GABA transporter GAT-1 Is modulated by its ligands. J Biol Chem 2004;279:13800–13808. [PubMed: 14744863]
30. Loland CJ, Norregaard L, Gether U. Defining proximity relationships in the tertiary structure of the dopamine transporter. Identification of a conserved glutamic acid as a third coordinate in the endogenous $Zn^{2+}$-binding site. J Biol Chem 1999;274:36928–36934. [PubMed: 10601246]
31. Schwartz TW, Frimurer TM, Holst B, Rosenkilde MM, Elling CE. Molecular mechanism of 7TM receptor activation—a global toggle switch model. Annu Rev Pharmacol Toxicol 2006;46:481–519. [PubMed: 16402913]
32. White KJ, Kiser PD, Nichols DE, Barker EL. Engineered zinc-binding sites confirm proximity and orientation of transmembrane helices I and III in the human serotonin transporter. Protein Sci 2006;15:2411–2422. [PubMed: 17008722]
33. Loland CJ, Granas C, Javitch JA, Gether U. Identification of intracellular residues in the dopamine transporter critical for regulation of transporter conformation and cocaine binding. J Biol Chem 2004;279:3228–3238. [PubMed: 14597628]
34. Zomot E, Zhou Y, Kanner BI. Proximity of transmembrane domains 1 and 3 of the GABA transporter GAT-1 inferred from paired cysteine mutagenesis. J Biol Chem 2005;280:25512–25516. [PubMed: 15905165]
35. Newman AH, Kulkarni S. Probes for the dopamine transporter: new leads toward a cocaine-abuse therapeutic—a focus on analogues of benztropine and rimcazole. Med Res Rev 2002;22:429–464. [PubMed: 12210554]
36. Desai RI, Kopajtic TA, Koffarnus M, Newman AH, Katz JL. Identification of a dopamine transporter ligand that blocks the stimulant effects of cocaine. J Neurosci 2005;25:1889–1893. [PubMed: 15728828]
37. Loland CJ, et al. Relationship between conformational changes in the dopamine transporter and cocaine-like subjective effects of uptake inhibitors. Mol Pharmacol 2008;73:813–823. [PubMed: 17978168]
38. Lin Z, Uhl GR. Dopamine transporter mutants with cocaine resistance and normal dopamine uptake provide targets for cocaine antagonism. Mol Pharmacol 2002;61:885–891. [PubMed: 11901228]
39. Chen R, Han DD, Gu HH. A triple mutation in the second transmembrane domain of mouse dopamine transporter markedly decreases sensitivity to cocaine and methylphenidate. J Neurochem 2005;94:352–359. [PubMed: 15998286]
40. Sen N, Shi L, Beuming T, Weinstein H, Javitch JA. A pincer-like configuration of TM2 in the human dopamine transporter is responsible for indirect effects on cocaine binding. Neuropharmacology 2005;49:780–790. [PubMed: 16216288]
41. Loland CJ, Norregaard L, Litman T, Gether U. Generation of an activating $Zn^{2+}$ switch in the dopamine transporter: mutation of an intracellular tyrosine constitutively alters the conformational equilibrium of the transport cycle. Proc Natl Acad Sci USA 2002;99:1683–1688. [PubMed: 11818545]
42. Barker EL, Moore KR, Rakhshan F, Blakely RD. Transmembrane domain I contributes to the permeation pathway for serotonin and ions in the serotonin transporter. J Neurosci 1999;19:4705–4717. [PubMed: 10366604]
43. Ravna AW, Sylte I, Dahl SG. Molecular model of the neural dopamine transporter. J Comput Aided Mol Des 2003;17:367–382. [PubMed: 14635728]
44. Edvardsen O, Dahl SG. A putative model of the dopamine transporter. Brain Res Mol Brain Res 1994;27:265–274. [PubMed: 7898310]
45. Katz JL, Kopajtic TA, Agoston GE, Newman AH. Effects of N-substituted analogues of benztropine: diminished cocaine-like effects in dopamine transporter ligands. J Pharmacol Exp Ther 2004;309:650–660. [PubMed: 14755006]
46. Brooks BR, et al. CHARMM: A program for macromolecular energy, minimization, and dynamics calculations. J Comput Chem 1983;4:187–217.

47. Bayly CI, Ceplak PDCW, Kollman PA. A well-behaved electrostatic potential–based method using charge restraints for deriving atomic charges: the RESP model. J Phys Chem 1993;97:10269–10280.

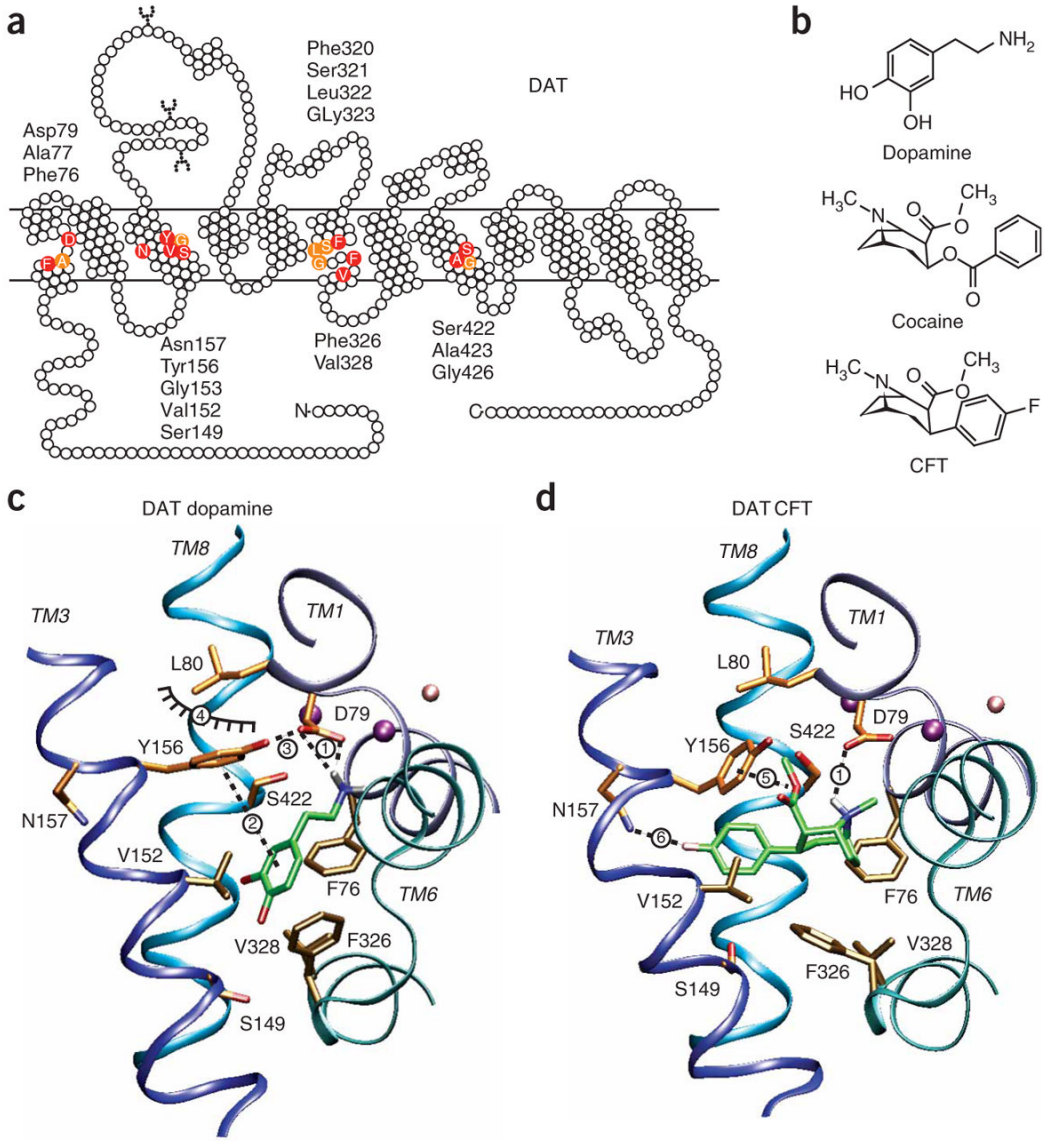


**Figure 1.**

Models of DAT/ligand complexes. (**a**) Two-dimensional schematic representation of the human dopamine transporter (hDAT). Colored circles indicate residues that interact with either dopamine or the cocaine analog CFT in the molecular models. Red circles indicate side-chain interaction and orange circles indicate backbone interaction. (**b**) Structure of dopamine, cocaine and CFT. (**c**,**d**) Docked dopamine (**c**) and CFT (**d**) in DAT. Transmembrane domains 1, 3, 6 and 8 are shown in various shades of blue; the other transmembrane domains and intra- and extracellular loops have been removed for clarity. The ligands are shown in green. Sodium and chloride ions are shown as purple and salmon spheres, respectively. Encircled numbers refer to the specific interactions motifs. Motif 1 (**c**), salt bridge interaction between Asp79 and the protonated amine of dopamine; motif 1 (**d**), polar interaction between Asp79 and the amine of CFT; motif 2, aromatic-aromatic stacking interaction between Tyr156 and the catechol ring of dopamine; motif 3, hydrogen bond between the OH group of Tyr156 and Asp79; motif 4, hydrophobic-aromatic interaction between Leu80 and Tyr156; motif 5, interaction between

Tyr156 and the 2β-methylester substituent of CFT; motif 6, interaction between the nitrogen of Asn157 and the fluoride atom of CFT.

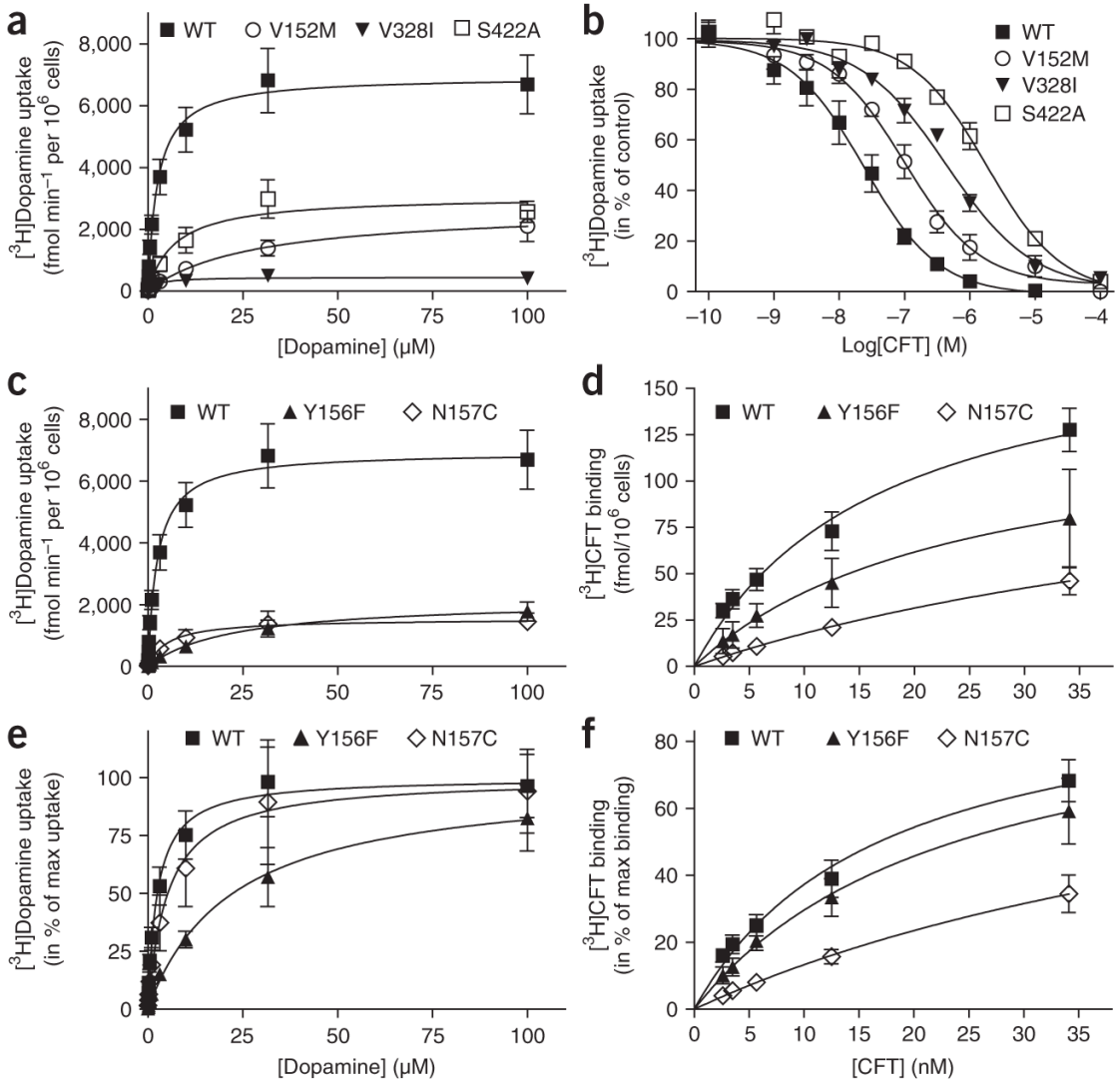


**Figure 2.**

Evidence for involvement of Val152, Tyr156, Asn157, Val328 and Ser422 in binding of dopamine and/or CFT by DAT. (**a**) [$^3$H]dopamine uptake (shown as saturation curve) in COS7 cells expressing wild-type DAT (■), V152M (○), V328I (▼) or S422A (□). (**b**) Inhibition of [$^3$H]dopamine uptake by CFT in COS7 cells expressing wild-type DAT (■), V152M (○), V328I (▼) or S422A (□). (**c**) [$^3$H]dopamine uptake (shown as saturation curve) in COS7 cells expressing wild-type DAT (■), Y156F(▲) or N157C (◇). (**d**) [$^3$H]CFT binding (shown as saturation curve) in COS7 cells expressing wild-type DAT (■), Y156F(▲) or N157C (◇). (**e**) [$^3$H]dopamine uptake (shown as saturation curve normalized to maximum uptake) in COS7 cells expressing wild-type DAT (■), Y156F(▲) or N157C (◇). (**f**) [$^3$H]CFT binding (shown as saturation curve normalized to maximum binding) in COS7 cells expressing wild-type DAT (■), Y156F(▲) or N157C (◇). All data are means ± s.e.m. of 3–8 experiments carried out in triplicate. The saturation curves shown are transformations of the [$^3$H]dopamine uptake and [$^3$H]CFT binding competition assays that were used for calculation of the $K_M$ and $V_{MAX}$ values for [$^3$H]dopamine and the $K_D$ and $B_{MAX}$ values for [$^3$H]CFT (Supplementary Table 1).

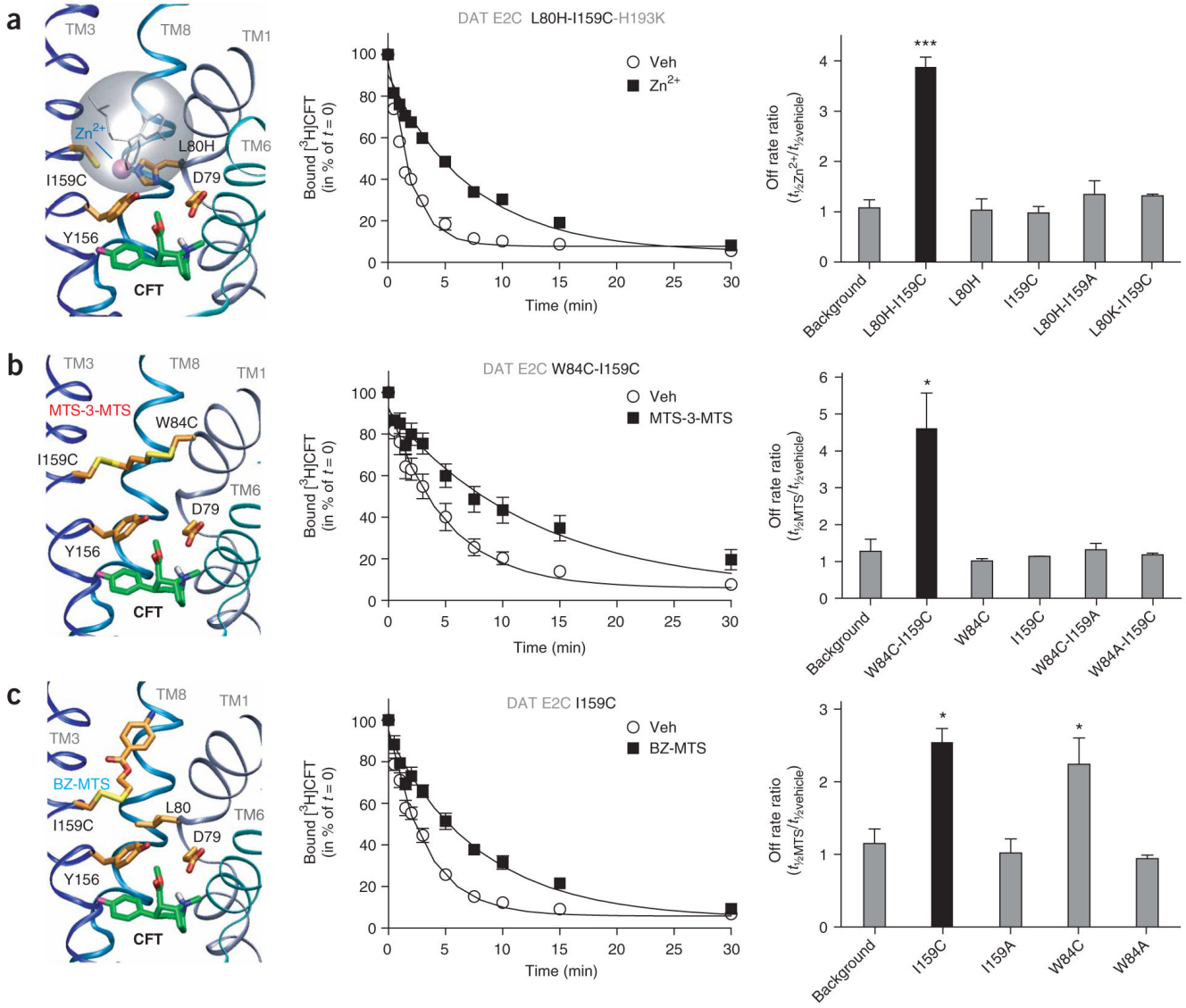


**Figure 3.**

Validation of the CFT docking model using intramolecular cross-linking and cysteine-reactive reagents. (**a**) Engineering of a $Zn^{2+}$-binding site between TMDs 1 and 3 in an extracellular vestibule above the predicted binding site resulted in partial trapping of [$^3$H]CFT in its binding site. Left, model of CFT docked into L80H-I159C with subsequent docking of a $Zn^{2+}$ ion in the site created by the mutated residues. $Zn^{2+}$ is shown as a purple sphere. The $Zn^{2+}$ binding site is positioned in the same locus of the transporter as the noncompetitive binding site for tricyclic antidepressants in LeuT[13,14] (illustrated by a spherical model of clomipramine bound to LeuT). CFT is shown in green. Middle, dissociation of prebound [$^3$H]CFT in COS7 cells expressing the double mutant L80H-I159C in the background construct E2C H193K with (■) or without (○) 100 μM $Zn^{2+}$. Right, effect of $Zn^{2+}$ (100 μM) on [$^3$H]CFT off-rate in the DAT background construct E2C H193K (named 'background') and in the mutations L80H-I159C, L80H, I159C, L80H-I159A or L80K-I159C (all made in E2C H193K). (**b**) Cysteine-mediated cross-linking between TMDs 1 and 3 resulted in partial trapping of [$^3$H]CFT in its binding site. Left, model of CFT docked into W84C-I159C with subsequent cross-linking of MTS-3-MTS. Middle, dissociation of prebound [$^3$H]CFT in COS7 cells expressing the double mutant W84C-

I159C in the E2C background with (■) or without (○) 0.5 mM MTS-3-MTS. Right, effect of 0.5 mM MTS-3-MTS on [$^3$H]CFT off-rate in the DAT background construct E2C (named 'background') and in the mutations W84C-I159C, W84C, I159C, W84C-I159A or W84A-I159C (all made in E2C). (**c**) Slower dissociation of [$^3$H]CFT by reacting I159C or W84C with the bulky MTS-reagent BZ-MTS. Left, model of CFT docked into I159C with subsequent reaction of I159C with BZ-MTS. Middle, dissociation of prebound [$^3$H]CFT in COS7 cells expressing the mutant I159C in the background construct E2C with (■) or without (○) 0.5 mM BZ-MTS. Right, effect of BZ-MTS on [$^3$H]CFT off-rate in the DAT background construct E2C (named 'background') and in the mutations I159C, I159A, W84C or W84A. All data in middle panels are percentages of bound [$^3$H]CFT at $t = 0$ (means ± s.e.m., $n$ =3–5). All data in right panels are the ratio between the $t½$ (min) for [$^3$H]CFT dissociation with and without $Zn^{2+}$ or MTS reagent (means ± s.e.m., $n = 3$). The [$^3$H]CFT off-rates ($t½$in min) in the absence of $Zn^{2+}$ or MTS reagent are given in the Supplementary Note. * $P < 0.05$), *** $P < 0.001$; one-way ANOVA with Newman-Keuls multiple comparison *post hoc* test.

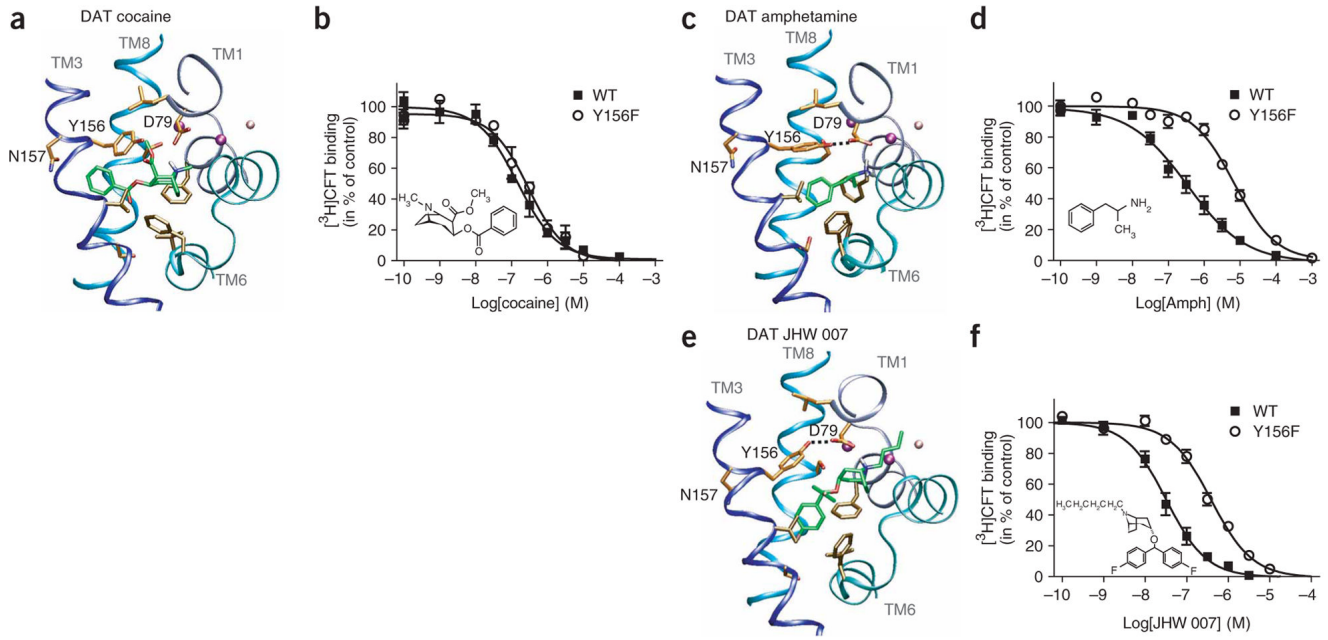


**Figure 4.**

Molecular docking models of cocaine, amphetamine (AMPH) and JHW007 with experimental validation. (**a**,**c**,**d**) Models of cocaine, amphetamine and JHW 007 docked in DAT, shown in the plane of the membrane. Transmembrane domains 1, 3, 6 and 8 are shown in various shades of blue; the other transmembrane domains and intra- and extracellular loops have been removed for clarity. The ligands are shown in green and interacting residues in yellow and brown. Sodium and chloride ions are shown in purple and salmon spheres, respectively. Note that the docking of cocaine does not allow the formation of a hydrogen bond between Asp79 and Tyr156, whereas both AMPH and JHW 007 allow this interaction to occur. (**b,d,f**) Inhibition of [$^3$H]CFT binding by cocaine (**b**), amphetamine (**d**) and JHW 007 (**f**) in COS7 cells expressing wild-type DAT (■) or DAT Y156F (○). Data are means ± s.e.m. of 3–4 experiments carried out in triplicate.

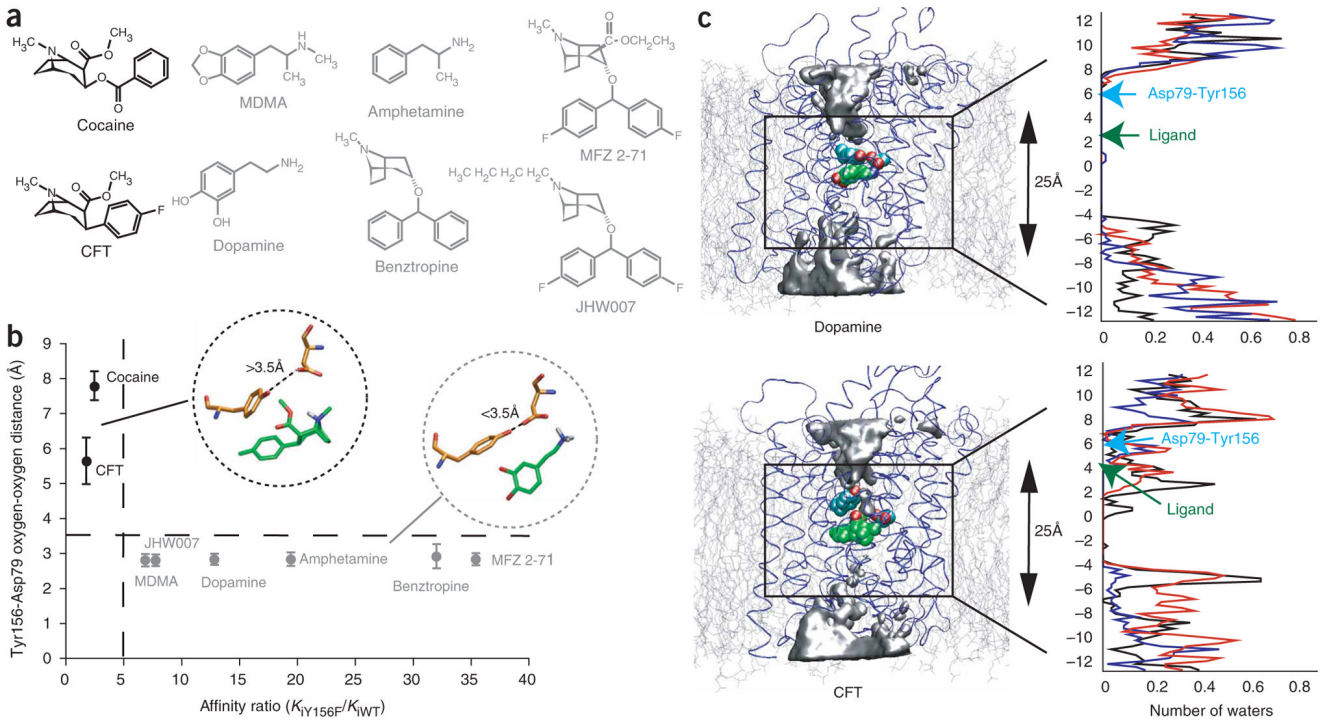


**Figure 5.**

Comparison of the CFT-binding mode with the binding mode of dopamine and other DAT ligands. (**a**) Chemical structures of all compounds docked into the DAT model. Compounds that hindered the Asp79-Tyr156 hydrogen bond when docked are shown in black; compounds that allowed the hydrogen bond are shown in gray. (**b**) Computationally estimated distance between the oxygen atoms of Tyr156 and Asp79 plotted against ligand Y156F/wild-type affinity ratio (values from Supplementary Table 2). The time-dependent behavior of the Tyr-Asp hydrogen bond was explored with molecular dynamics simulations. The hydrogen bond was continuously present (distance <3.5 Å) in all trajectories (gray) except for those of CFT and cocaine (black). Error bars are standard deviations of the estimated distances. Dotted lines indicate the minimal distance for hydrogen-bond formation (3.5 Å, horizontal) or an arbitrary fivefold affinity ratio (vertical). Inset, model of the Tyr-Asp interaction seen for the two classes of ligands. (**c**) Rendering of water permeation into the dopamine- (top) and CFT-binding (bottom) sites. Right, the distribution of water shown over a 25 Å distance along the membrane normal in the region indicated on the left by the rectangular box. The distribution was calculated from the last 5 ns of each of three separate simulations carried out for each ligand-DAT complex (red, blue and black traces, respectively). The locations of the geometric centers of Tyr156 and Asp79 and ligands at the end of the simulations are indicated by blue and green arrows, respectively, and water molecule numbers are indicated as a function of distance. Left, water distribution in context of the structure; silver-colored surfaces indicate the water penetration, with the structures of Tyr156, Asp79 and the ligands rendered.

**Table 1**

Interactions in the DAT model with dopamine and CFT

| Residues | | Dopamine | | | CFT | | |
|---|---|---|---|---|---|---|---|
| | | Contact | Interaction | SC/BB | Contact | Interaction | SC/BB |
| PHE | 76 | x | Ring + Amine | SC + BB | x | Tropane + Amine | SC + BB |
| ALA | 77 | x | Amine | BB | x | *N*-met | BB |
| ASP | 79 | x | Amine | SC | x | Amine | SC |
| SER | 149 | x | OH | SC + BB | x | Arom | BB |
| VAL | 152 | x | Ring | SC | x | Arom | SC + BB |
| GLY | 153 | | | | x | Arom | BB |
| TYR | 156 | x | Ring | SC | x | Methyl ester | SC + BB |
| ASN | 157 | | | | x | Fluorine | SC + BB |
| PHE | 320 | x | Ring + Amine | SC + BB | x | Tropane | SC + BB |
| SER | 321 | x | Amine | BB | x | *N*-met | BB |
| LEU | 322 | x | Amine | BB | x | *N*-met | BB |
| GLY | 323 | x | Ring | BB | x | *N*-met | BB |
| PHE | 326 | x | Ring | SC | x | Tropane | SC |
| VAL | 328 | x | Ring | SC | x | Tropane | SC |
| SER | 422 | x | OH | SC + BB | x | Arom | SC + BB |
| ALA | 423 | x | OH | BB | x | Arom | SC + BB |
| GLY | 426 | x | OH | BB | x | Arom | BB |

All residues within 4 Å of the ligand during the molecular dynamics trajectory are shown. Arom, aromatic ring; BB, backbone; SC, side chain.